

Mathematical modeling of pollutant transport in river Fena in Ghana

Ferdinand Obeng-Forson¹, Joseph K. Ansong^{1*}

¹Department of Mathematics, University of Ghana, Legon, Ghana.

*Corresponding Author: jkansong@ug.edu.gh

Abstract

In this study, we derived two analytical solutions to a one-dimensional Advection-Diffusion Equation (ADE). The ADE is solved using a constant and exponentially decaying inlet boundary condition, together with Dirichlet and Neumann outlet conditions. The analytic solutions are shown to be simple if a combination of the initial concentration and the transformed boundary condition results in a non-zero singularity pole of inverse Laplace transform. The differences between the two analytic solutions are elucidated. Moreover, the analytical solutions are compared to some observational data from the Fena River in the Ashanti region of Ghana where illegal mining activities (locally referred to as “galamsey”) have been reported. The analytical results well capture the concentration of iron at two sampling locations for both the Dirichlet and Neumann models but poorly predict the concentration at a third location. Some possible reasons for this discrepancy have been hypothesized for future investigations.

Introduction

Water is essential to our existence and survival and its importance cannot be overstated. Rivers, being the most significant sources of water, are the lifeblood of humans. Not only does a river act as a primary source of irrigation for the majority of agricultural communities across the globe, but it also supplies clean and fresh water for daily necessities of living.

One major issue that poses a serious threat to both human life and the aquatic ecosystem is water pollution. Water pollution occurs when hazardous substances, such as chemicals or microbes, infiltrate an ocean, lake, stream, aquifer, or a river body, deteriorating water quality and making it harmful to humans or the environment. According to the Ghana Water Resource Commission, nearly 60% of water bodies in Ghana are polluted due to illegal mining and inappropriate agriculture methods (Mubarik, 2017). The discharge of waste substances, which contain hazardous compounds such as mercury and other organic chemicals used in mineral ores processing in mining activities. These waste substances contribute heavily to water pollution

in Ghana, posing a greater threat to aquatic life and the human population that relies on such resources (Duncan et al., 2020). According to the Ministry of Lands and Natural resources, Ghana risks importing water as illegal miners devastate the country’s rivers (Ghanaian Times, 2022). Once river bodies become polluted it is extremely difficult to clean up.

The transport of pollutants in rivers has become a matter of concern for environmental engineers and scientists as well as mathematical modelers. The effective control of these pollutants is critical for efficient management of their impact on the environment (Zoppou & Knight, 1997). The concentration of these pollutants released into water bodies may be described by an Advection-Diffusion Equation (ADE), a partial differential equation of parabolic type. The ADE describes a physical phenomenon whereby contaminants or other unwanted substances are transported inside a physical system due to two processes: advection and diffusion. The ADE has extensively been used to model water pollution phenomenon (Schaffner et al., 2009, Genuchten et al., 2013, Manitcharoen & Pimpunchat, 2020). It also has

a wide range of applications in many engineering fields such as modeling atmospheric pollutants (Costa et al., 2006, Moreira et al., 2006), tracer dispersion in a porous medium (Ogata & Banks 1961), and the intrusion of salt water into freshwater aquifers (Essink, 2001).

Obtaining analytic solutions to the Advection-Diffusion Equation is of great importance in mathematics. Analytical solutions are especially critical for validating solutions of the ADE obtained using numerical methods. Many analytical solutions along with varying initial and boundary conditions have been developed to quantitatively describe the one-dimensional ADE with constant coefficients. A one-dimensional (1D) single-ion ADE, which involves terms accounting for zero-order production, linear equilibrium adsorption, and first-order decay, was solved analytically by Van Genuchten (1982). Mohsen and Baluch (1983) provided an analytic solution to a 1D ADE for fixed concentration boundary conditions over a finite domain. The transformed equation was decomposed into two components and separation of variables was used to obtain the required result. Davis (1985), using a Laplace transform technique, provided two distinct analytic solutions to a single ADE over a finite domain. One solution was found to be continuous at both ends of the domain, and the other is discontinuous at the origin. In order to resolve the discontinuity at the origin, he compared the discontinuous analytic solution to the one provided by Mohsen and Baluch (1983) in Eq (20) of his paper. He found that his results and that of Mohsen and Baluch (1983) were the same but was incorrectly given as the negative of his solution. He stated that the discontinuity at the origin in the equation was due to the Fourier sine series expansion for the ratio of hyperbolic sines. In a semi-infinite domain where the diffusion coefficient is proportional to the square of the spatially dependent velocity, Kumar et al., (2012) presented an analytic solution to a 1D ADE with variable coefficients using the Laplace transform technique. Mojtabi and Deville (2015) also provided an analytical solution to a one-dimensional ADE using separation of variables but with a sinusoidal initial condition and a homogeneous boundary condition. Using a one-sided Laplace transform, Kim (2020) provided analytic solutions to a 1D Convection-Diffu-

sion Reaction Source (CDRS) equation without explicitly computing the inverse Laplace transform. The CDRS equation was solved for both Dirichlet/Dirichlet and Dirichlet/Neumann boundary conditions together with a constant initial condition. Unlike most previous research on the ADE, few have provided analytical solutions to a one-dimensional ADE subject to an exponentially decaying boundary condition.

This paper presents analytic solutions to a one-dimensional ADE using constant initial condition and an exponentially decaying inlet boundary condition, together with Dirichlet and Neumann outlet conditions. Without directly computing the inverse Laplace transform, solutions to the ADE are obtained using the Laplace transform technique and the residue theorem approach in complex analysis as employed in Kim (2020). Additionally, the analytical solutions are compared to some observational data and the differences between the two are discussed.

Background Theory

The one-dimensional Advection-Diffusion Equation, with constant coefficients which is derived from the principle of mass conservation, is given by

$$\frac{\partial C}{\partial t} + V_0 \frac{\partial C}{\partial x} = D_0 \frac{\partial^2 C}{\partial x^2}, \quad (1)$$

where C is the concentration at a position, x and time t , and V_0 and D_0 are the constant advective velocity and diffusion, respectively. Using the dimensionless quantities defined by

$$\phi(\xi, \tau) = C(x, t)/C_0, \quad \tau = tD_0/L^2,$$

$$\xi = x/L, \quad P_e = 2\lambda = LV_0/D_0,$$

where C_0 is a reference concentration, L is a length scale of the space coordinate and $P_e = 2\lambda$ is the Peclet number, the dimensionless form of the ADE in Eq. (1) becomes

$$\frac{\partial \phi}{\partial \tau} = \frac{\partial^2 \phi}{\partial \xi^2} - 2\lambda \frac{\partial \phi}{\partial \xi} \tag{2}$$

We next introduce and discuss two analytical solutions to the 1D ADE with Dirichlet boundary condition (referred to as Dirichlet Model) and Neumann boundary condition (referred to as Neumann Model).

Dirichlet Model

The equation to be solved is

$$\frac{\partial \phi}{\partial \tau} = \frac{\partial^2 \phi}{\partial \xi^2} - 2\lambda \frac{\partial \phi}{\partial \xi}, \quad 0 \leq \xi \leq 1, \tag{3}$$

subject to boundary conditions (BCs):

$$\dot{\phi}(0, \tau) = \phi_0 e^{-\gamma \tau}, \tag{4}$$

$$\phi(1, \tau) = \phi_1,$$

and initial condition

$$\phi(\xi, 0) = \omega_0. \tag{5}$$

The choice of the exponentially decaying inlet BC is motivated by observational data in Fena River in Ghana (Duncan et al., 2020), where the pollutant at the inlet appears to be decaying in time as shown later.

Applying the Laplace transform

$$\Phi(\xi, p) := \mathcal{L}[\phi(\xi, \cdot)](p) = \int_0^\infty e^{-p\tau} \phi(\xi, \tau) d\tau \tag{6}$$

to Eq. (3) gives a second order ordinary differential equation

$$\frac{d^2 \Phi}{d\xi^2} - 2\lambda \frac{d\Phi}{d\xi} - p\Phi = -\omega_0 \tag{7}$$

$$[\mathcal{D}_\xi - \lambda_m][\mathcal{D}_\xi - \lambda_p]\Phi = -\omega_0, \tag{8}$$

where

$$\mathcal{D}_\xi = \frac{d}{d\xi}, \quad \lambda_m = \lambda - \beta, \quad \lambda_p = \lambda + \beta \quad \text{and} \quad \beta = \sqrt{\lambda^2 + p}.$$

Define a new function as:

$$\Phi^\dagger := [\mathcal{D}_\xi - \lambda_p]\Phi = e^{\lambda_p \xi} \mathcal{D}_\xi(\Phi e^{-\lambda_p \xi}). \tag{9}$$

We now write Eq. (8) as

$$e^{\lambda_m \xi} \mathcal{D}_\xi(\Phi^\dagger e^{-\lambda_m \xi}) = -\omega_0. \tag{10}$$

The general solution for Φ^\dagger is

$$\Phi^\dagger = B_1 e^{\lambda_m \xi} + \frac{\omega_0}{\lambda_m}. \tag{11}$$

Substituting Eq. (11) into Eq. (9) gives the general solution for $\Phi(\xi, p)$ as

$$\Phi(\xi, p) = B_1 e^{\lambda_m \xi} + B_2 e^{\lambda_p \xi} + \frac{\omega_0}{p} \tag{12}$$

where

$$\Phi(0, p) = \frac{\phi_0}{p + \gamma} \quad \text{and} \quad \Phi(1, p) = \frac{\phi_1}{p}. \tag{13}$$

Applying Eq. (13) above to Eq. (12) gives

$$B_1 = \frac{\left(\frac{\phi_0}{p + \gamma} - \frac{\omega_0}{p}\right) e^\beta - \left(\frac{\phi_1}{p} - \frac{\omega_0}{p}\right) e^{-\lambda}}{2 \sinh \beta}, \tag{14}$$

$$B_2 = \frac{\left(\frac{\phi_1}{p} - \frac{\omega_0}{p}\right) e^{-\lambda} - \left(\frac{\phi_0}{p + \gamma} - \frac{\omega_0}{p}\right) e^{-\beta}}{2 \sinh \beta}. \tag{15}$$

Substituting the values of B_1 and B_2 into Eq. (12) gives the general solution in terms of p as

$$\Phi(\xi, p) = \left[\frac{\phi_0 \sinh[\beta(1 - \xi)]}{\sinh \beta} \right] \frac{e^{\lambda \xi}}{p + \gamma} + \left[\frac{\phi_1 e^{-\lambda} \sinh(\beta \xi)}{\sinh \beta} \right] \frac{e^{\lambda \xi}}{p}$$

$$- \left[\frac{\omega_0 \sinh [\beta(1 - \xi)] + \omega_0 e^{-\lambda} \sinh(\beta\xi)}{\sinh \beta} \right] \frac{e^{\lambda\xi}}{p} + \frac{\omega_0}{p}. \quad (16)$$

To solve Eq. (16), one must apply the inverse Laplace transform (iLT) defined below which involves the method of contour integration and calculus of residues.

$$\phi(\xi, \tau) = \mathcal{L}^{-1}[\Phi(\xi, \cdot)](\tau) = \frac{1}{2\pi i} \int_{c-i\infty}^{c+i\infty} e^{\tau z} \Phi(\xi, z) dz.$$

However, this approach is most often difficult to use. Here, we apply the method devised by Kim (2020) which states that if a Laplace transformed function has only two singularity poles, $z = z_0$ (contributing to the steady-state solution) and $z = z_1$ (contributing to the transient behaviour), then the inverse Laplace transform can be avoided by applying the initial condition. To apply this method, we first let

$$\Phi_{BC}(\xi, p) = \left[\frac{\phi_0 \sinh [\beta(1 - \xi)]}{\sinh \beta} \right] \frac{e^{\lambda\xi}}{p + \gamma} + \left[\frac{\phi_1 e^{-\lambda} \sinh(\beta\xi)}{\sinh \beta} \right] \frac{e^{\lambda\xi}}{p}$$

$$\Phi_{IC}(\xi, p) = - \left[\frac{\omega_0 \sinh [\beta(1 - \xi)] + \omega_0 e^{-\lambda} \sinh(\beta\xi)}{\sinh \beta} \right] \frac{e^{\lambda\xi}}{p} + \frac{\omega_0}{p},$$

and also let

$$\Phi_{BC_1}(\xi, p) = \left[\frac{\phi_0 \sinh [\beta(1 - \xi)]}{\sinh \beta} \right] \frac{e^{\lambda\xi}}{p + \gamma},$$

$$\Phi_{BC_2}(\xi, p) = \left[\frac{\phi_1 e^{-\lambda} \sinh(\beta\xi)}{\sinh \beta} \right] \frac{e^{\lambda\xi}}{p},$$

where Φ_{BC_1} , Φ_{BC_2} and Φ_{IC} are partial solutions of Φ . We replace the Laplace parameter p by the complex variable z and write the iLT of Eq. (16) as

$$\begin{aligned} \phi(\xi, \tau) &= \mathcal{L}^{-1}[\Phi(\xi, \cdot)](\tau) = \frac{1}{2\pi i} \int_{c-i\infty}^{c+i\infty} e^{\tau z} \Phi(\xi, z) dz \\ &= \text{Res}[\exp(\tau z) \Phi_{BC_1}(\xi, z) + \exp(\tau z) \Phi_{BC_2}(\xi, z) + \exp(\tau z) \Phi_{IC}(\xi, z)]. \end{aligned}$$

The expressions $\exp(\tau z)\Phi_{BC_1}(\xi, z)$, $\exp(\tau z)\Phi_{BC_2}(\xi, z)$ and $\exp(\tau z)\Phi_{IC}(\xi, z)$ have simple poles at $z = 0$ and $z = -\gamma$.

The Residue of $\exp(\tau z)\Phi_{BC}(\xi, z)$ and $\exp(\tau z)\Phi_{IC}(\xi, z)$ at the simple poles are calculated as follows:

$$\text{Res}(\Phi, z = -\gamma) = \lim_{z \rightarrow -\gamma} [(z + \gamma)\Phi_{BC_1}(\xi, z)e^{\tau z}] = f_{B_1} e^{\lambda\xi - \gamma\tau},$$

where

$$f_{B_1} = \left[\frac{\phi_0 \sinh \omega(1 - \xi)}{\sinh \omega} \right] \tag{17}$$

and $\omega = \sqrt{\lambda^2 - \gamma}$. For physically relevant solutions, we suppose that $\lambda^2 > \gamma$. Solutions for the case where $\lambda^2 < \gamma$ can be derived (see Obeng-Forson, 2022) but yield unrealistic values.

Similarly,

$$\text{Res}(\Phi, z = 0) = \lim_{z \rightarrow 0} [z\Phi_{BC_2}(\xi, z)e^{\tau z}] = f_{B_2} e^{\lambda\xi},$$

where

$$f_{B_2} = \left[\frac{\phi_1 e^{-\lambda} \sinh(\lambda \xi)}{\sinh \lambda} \right]. \tag{18}$$

Also,

$$\text{Res}(\Phi, z = 0) = \lim_{z \rightarrow 0} [z\Phi_{IC}(\xi, z)e^{\tau z}] = -f_C e^{\lambda\xi} + \omega_0,$$

where

$$f_C = \frac{\omega_0 \sinh[\lambda(1 - \xi)] + \omega_0 e^{-\lambda} \sinh(\lambda\xi)}{\sinh \lambda}. \tag{19}$$

Besides, $\Phi_{BC}(\xi, z)$ and $\Phi_{IC}(\xi, z)$ have the same pole when

$$\sinh \beta = 0 \implies z = -\lambda^2.$$

The Residues at $z = -\lambda^2$ are calculated below. That of $\exp(\tau z)\Phi_{BC_1}(\xi, z)$ is calculated as

$$\lim_{z \rightarrow -\lambda^2} [(z + \lambda^2)e^{\tau z}\Phi_{BC_1}(\xi, z)] = -\frac{e^{\lambda\xi - \lambda^2\tau}}{\lambda^2 - \gamma} \mathcal{R}[f_{B_1}],$$

where

$$\mathcal{R}[f_{B_1}] = \lim_{z \rightarrow -\lambda^2} (z + \lambda^2) \left(\frac{\phi_0 \sinh \beta(1 - \xi)}{\sinh \beta} \right)$$

and $\beta = \sqrt{\lambda^2 + z}$.

Similarly, the Residue of $\exp(\tau z)\Phi_{BC_2}(\xi, z)$ is calculated as

$$\lim_{z \rightarrow -\lambda^2} [(z + \lambda^2)e^{\tau z}\Phi_{BC_2}(\xi, z)] = -\frac{e^{\lambda\xi - \lambda^2\tau}}{\lambda^2} \mathcal{R}[f_{B_2}]$$

where

$$\mathcal{R}[f_{B_2}] = \lim_{z \rightarrow -\lambda^2} (z + \lambda^2) \left(\frac{\phi_1 e^{-\lambda} \sinh(\beta \xi)}{\sinh \beta} \right).$$

Lastly, the residue of $\exp(\tau z)\Phi_{IC}(\xi, z)$ is

$$\lim_{z \rightarrow -\lambda^2} [(z + \lambda^2)e^{\tau z}\Phi_{IC}(\xi, z)] = \frac{e^{\lambda\xi - \lambda^2\tau}}{\lambda^2} \mathcal{R}[f_C]$$

where

$$\mathcal{R}[f_C] = \lim_{z \rightarrow -\lambda^2} (z + \lambda^2) \left(\frac{\omega_0 \sinh[\beta(1 - \xi)] + \omega_0 e^{-\lambda} \sinh(\beta\xi)}{\sinh \beta} \right)$$

and $\mathcal{R}[f]$ indicates the specific residue to be calculated for $z = -\lambda^2$.

Using the calculated residues, the solution can now be written in terms of τ as

$$\begin{aligned} \phi(\xi, \tau) = & f_{B_1} e^{\lambda\xi - \gamma\tau} + f_{B_2} e^{\lambda\xi} - f_C e^{\lambda\xi} - (\lambda^2 - \gamma)^{-1} e^{\lambda\xi - \lambda^2\tau} \mathcal{R}[f_{B_1}] \\ & - \lambda^{-2} e^{\lambda\xi - \lambda^2\tau} \mathcal{R}[f_{B_2}] + \lambda^{-2} e^{\lambda\xi - \lambda^2\tau} \mathcal{R}[f_C] + \omega_0 \end{aligned} \quad (20)$$

where the residues $\mathcal{R}[f]$ are still unknown.

A major step in the solution approach is to apply the initial condition $\phi(\xi, 0) = \omega_0$ to Eq.(20) to calculate for the residues.

This gives

$$(\lambda^2 - \gamma)^{-1} \mathcal{R}[f_{B_1}] + \lambda^{-2} \mathcal{R}[f_{B_2}] - \lambda^{-2} \mathcal{R}[f_C] = f_{B_1} + f_{B_2} - f_C, \quad (21)$$

and substituting Eq. (21) into Eq. (20) gives

$$\begin{aligned}\phi(\xi, \tau) &= f_{B_1} e^{\lambda\xi - \gamma\tau} + f_{B_2} e^{\lambda\xi} - f_C e^{\lambda\xi} - (f_{B_1} + f_{B_2} - f_C) e^{\lambda\xi - \lambda^2\tau} + \omega_0 \\ &= f_{B_1} [e^{-\gamma\tau} - e^{-\lambda^2\tau}] e^{\lambda\xi} + f_{B_2} [1 - e^{-\lambda^2\tau}] e^{\lambda\xi} - f_C [1 - e^{-\lambda^2\tau}] e^{\lambda\xi} + \omega_0\end{aligned}\quad (22)$$

Substituting Eq. (17), Eq. (18) and Eq. (19) into Eq. (22) yields

$$\begin{aligned}\phi(\xi, \tau) &= \frac{\phi_0 \sinh \omega(1 - \xi)}{\sinh \omega} [e^{-\gamma\tau} - e^{-\lambda^2\tau}] e^{\lambda\xi} + \frac{\phi_1 e^{-\lambda} \sinh(\lambda\xi)}{\sinh \lambda} [1 - e^{-\lambda^2\tau}] e^{\lambda\xi} \\ &\quad - \omega_0 \left(\frac{\sinh \lambda(1 - \xi) + e^{-\lambda} \sinh(\lambda\xi)}{\sinh \lambda} \right) [1 - e^{-\lambda^2\tau}] e^{\lambda\xi} + \omega_0.\end{aligned}\quad (23)$$

The steady-state solution for $\phi(\xi, \tau)$ is given as

$$\phi_{ss}(\xi) = \frac{\phi_1 e^{-\lambda} \sinh(\lambda\xi)}{\sinh \lambda} e^{\lambda\xi} - \omega_0 \left(\frac{\sinh \lambda(1 - \xi) + e^{-\lambda} \sinh(\lambda\xi)}{\sinh \lambda} \right) e^{\lambda\xi} + \omega_0$$

The solution for $\phi(\xi, \tau)$ holds for $0 < \xi < 1$ but it does not satisfy the conditions at the boundaries in general. However, it can be shown that to satisfy the inlet boundary condition, we must have $\omega_0 = \phi_0$. Similarly, to satisfy only the outlet condition one must have $\omega_0 = \phi_1$.

When $\gamma = 0$ we recover the general solution provided by Kim (2020) (Eq. (8) in his paper for $\kappa = 0$ and $\sigma = 0$.)

Figure 1 shows plots of Eq. (23) for fixed values of τ . When $\gamma = 0$, we recover the solution of Kim (2020) as displayed in Figure 1A. In this case, the concentration everywhere within the domain increases with time until the system reaches steady state, with concentration decreasing monotonically from the inlet to the outlet.

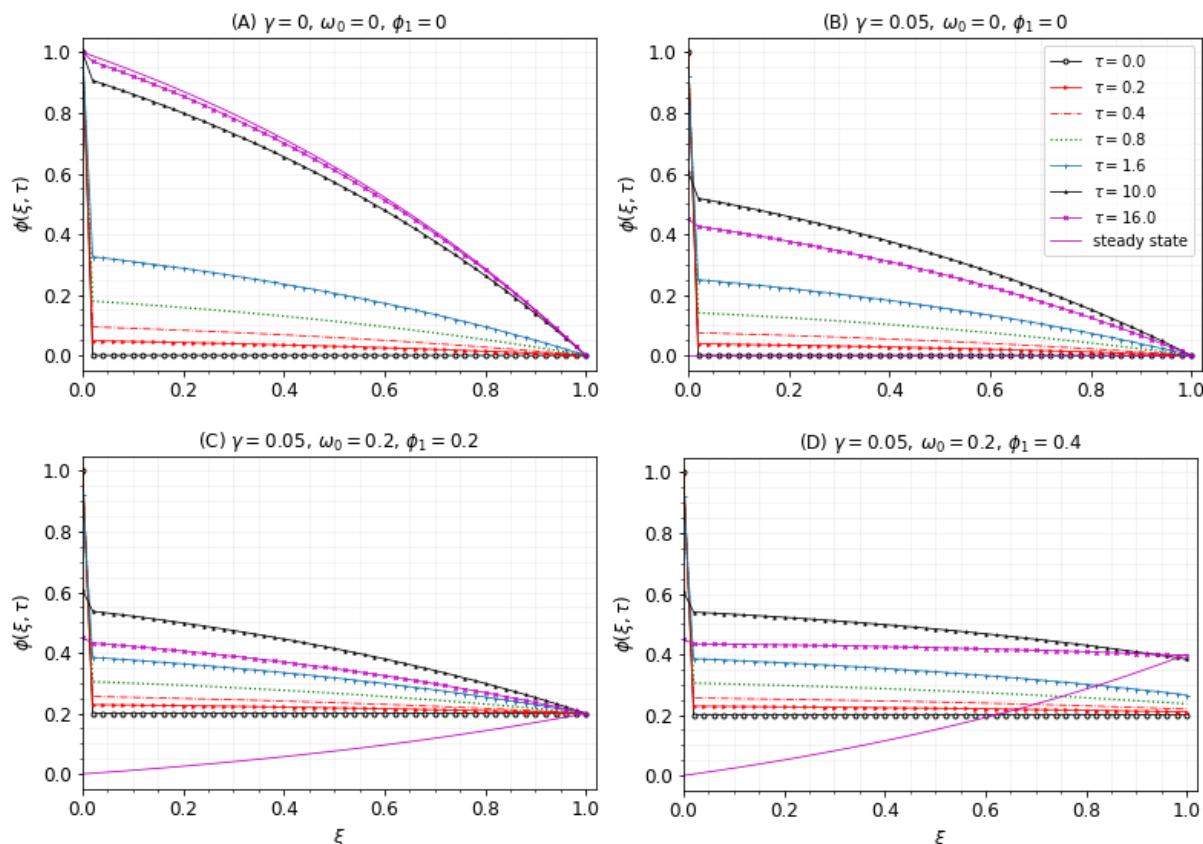


Figure 1: Concentration at different times for $\lambda = 0.5$, $\phi_0 = 1$ and (A) $\gamma = 0, \omega_0 = 0 = \phi_1$ (B) $\gamma = 0.05, \omega_0 = 0 = \phi_1$ (C) $\gamma = 0.05, \omega_0 = 0, \phi_1 = 0.2$ and (D) $\gamma = 0.05, \omega_0 = 0.2, \phi_1 = 0.4$.

However, in the presence of a decaying inlet condition with a Dirichlet outlet condition, the time evolution of concentration behaves differently from the case for which $\gamma = 0$ as seen in Figure 1B. Initially the concentration is zero except at the inlet where it has a maximum value of $\phi(\xi, 0) = \phi_0 = 1$. As time evolves, the concentration at the inlet begins to decrease while the concentration everywhere within the domain increases, with a monotonically decreasing shape as in Figure 1A. The concentration within the domain increases to a maximum point (around $\tau = 10$ in this case) and begins to decrease (see the curve for $\tau = 16$) and eventually goes to zero everywhere at steady-state.

If both the initial concentration and γ are non-zero (e.g., $\omega_0 = \phi_1 = 0.2, \gamma = 0.05$), the solution behaves similarly to the case for $\omega_0 = 0$ (Figure 1B), but the rate of increase of ϕ within the domain to the maximum point is much faster (Figure 1C), since the initial concentration is non-zero. Moreover, the steady state solution is not zero everywhere as in the previous case but increases gradually from zero at the inlet to the value at the outlet. Thus, in

this case, the concentration can decrease below the initial concentration due to the exponentially decreasing condition at the inlet. A more general case in which the initial condition and outlet value are non-zero and different from each other is shown in Figure 1D. The concentration increases to a maximum value as in Figures 1B-C, but tends to converge at the outlet value ($\phi_1 = 0.4$ in this case).

Neumann Model

The equation to be solved is

$$\frac{\partial \phi}{\partial \tau} = \frac{\partial^2 \phi}{\partial \xi^2} - 2\lambda \frac{\partial \phi}{\partial \xi}, \quad 0 \leq \xi \leq 1,$$

subject to BCs

$$\phi(0, \tau) = \phi_0 e^{-\gamma \tau}, \quad (24)$$

$$\frac{\partial \phi(1, \tau)}{\partial \xi} = J_1,$$

and initial condition

$$\phi(\xi, 0) = \omega_0. \quad (25)$$

Using the same procedure as in the Dirichlet model, the analytical solution to the Neumann model is (Obeng-Forson, 2022)

$$\begin{aligned} \phi(\xi, \tau) = & \frac{J_1 e^{-\lambda} \sinh \lambda \xi}{\lambda \sinh \lambda + \lambda \cosh \lambda} \left[1 - e^{-\lambda^2 \tau} \right] e^{\lambda \xi} \\ & + \frac{\phi_0 \lambda \sinh \omega(1 - \xi) + \phi_0 \omega \cosh \omega(1 - \xi)}{\lambda \sinh \omega + \omega \cosh \omega} \left[e^{-\gamma \tau} - e^{-\lambda^2 \tau} \right] e^{\lambda \xi} \\ & - \frac{\omega_0 \lambda \sinh \lambda(1 - \xi) + \omega_0 \lambda \cosh \lambda(1 - \xi)}{\lambda \sinh \lambda + \lambda \cosh \lambda} \left[1 - e^{-\lambda^2 \tau} \right] e^{\lambda \xi} + \omega_0. \end{aligned} \quad (26)$$

The steady-state solution is given as

$$\phi_{ss}(\xi) = \left(\frac{J_1 e^{-\lambda} \sinh \lambda \xi}{\lambda \sinh \lambda + \lambda \cosh \lambda} \right) e^{\lambda \xi} - \left(\frac{\omega_0 \lambda \sinh \lambda(1 - \xi) + \omega_0 \lambda \cosh \lambda(1 - \xi)}{\lambda \sinh \lambda + \lambda \cosh \lambda} \right) e^{\lambda \xi} + \omega_0. \quad (27)$$

Example plots from the solution in equations (26) and (27) can be found in Obeng-Forson (2022).

Application to the Transport of a Pollutant

We now apply our theoretical solutions to model the transport of a pollutant (iron) in the Fena River in the Ashanti region of Ghana.

Data are obtained from the published paper by Duncan et al., (2020) who conducted research in and around the Fena River to determine the levels of heavy metal pollution due to illegal mining (locally referred to as “galamsay”) activities. They took samples from five locations: Fenaso No. 1 (referred to as Fen-1), Fenaso No. 2 (referred to as Fen-2), Point A, Point B, Point C, and Fenaso No. 3 (referred to as Fen-3), in that order from north to south. Thus, the river flows southward from Fen-1 through Fen-3 until it enters the Gulf of Guinea in the Atlantic Ocean. A map of the area and sampling points can be seen in their Figure 1. The sampling points at Fen-1 and Fen-2 are very close to each other. According to Duncan et al., (2020), there were illegal mining activities in and around all the sampling locations except sampling Point A where there was no apparent mining activity

going on. The three main heavy metal pollutants in the river; exceeding safe drinking water guidelines, were found to be Cadmium (Cd), Lead (Pb) and Iron (Fe) (Duncan et al., 2020). Here, we focus on modeling the transport of Iron, because the initial and boundary data roughly match our theoretical set up.

The monthly concentration of Iron at three locations (Fen-1, Fen-2 and Point-A, obtained from Table 3 of Duncan et al., 2020) over the one-year period of their study (from January to December in 2020) is shown in Figure 2. We display only three locations because we are interested in modeling concentrations at Fen-2 and Point-A. We are particularly interested in Point-A because it was reported that there was no apparent illegal mining activity at the location, so we assume that the concentration of Fe at Point-A is likely due to upstream effects. The highest concentrations occur at Fen-1 and Fen-2 with the smallest concentrations of Fe at Point-C (not shown). The concentration of Fe at Fen-1 is generally decreasing with time over the study period (Figure 2a).

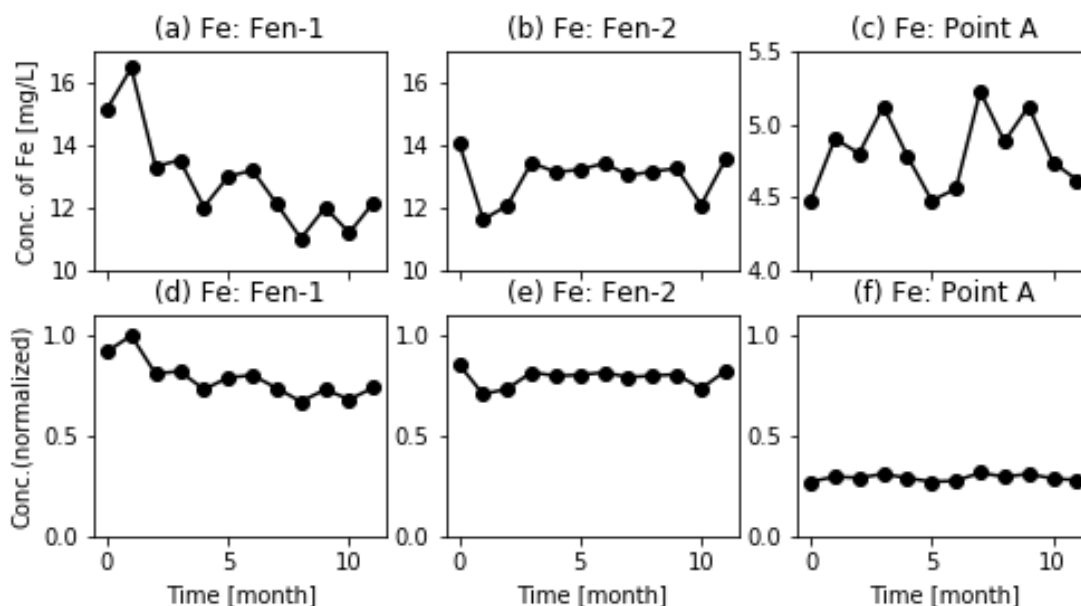


Figure 2 [Row 1] Variation of Iron (Fe) concentration over time in Fena river (as reported in Table 3 of Duncan et al., 2020). The vertical scales are different to highlight variability in concentrations. [Row 2] Same as Row 1 but for normalized concentrations.

Methodology and diffusion coefficient estimation

To apply our mathematical models, we normalized the concentrations by the highest concentration at Fen-1 (see Figure 3). The concentration at the inlet is taken to be the concentrations at Fen-1 while the initial concentration is taken to be that of January at all locations. The measured concentration of Fe in January is depicted in Figure 3 (left panel).

The parameter λ in the governing equation is related to the Peclet number $Pe = 2\lambda$ with $\lambda = LV_0/D_0$, where L is the length scale of the domain, V_0 is the averaged velocity of the flow and D_0 is a constant diffusion coefficient. We estimated the velocity, V_0 of the river to be 2m/s, by taking videos of the flow and measuring the speed of floating objects. We also measured the average width, W of the river around the same location to be ~ 5.2 m and the average depth, H to be 1.0 m. So, the average discharge, $Q = HWV_0$, at the location is about $10.4\text{m}^3/\text{s}$.

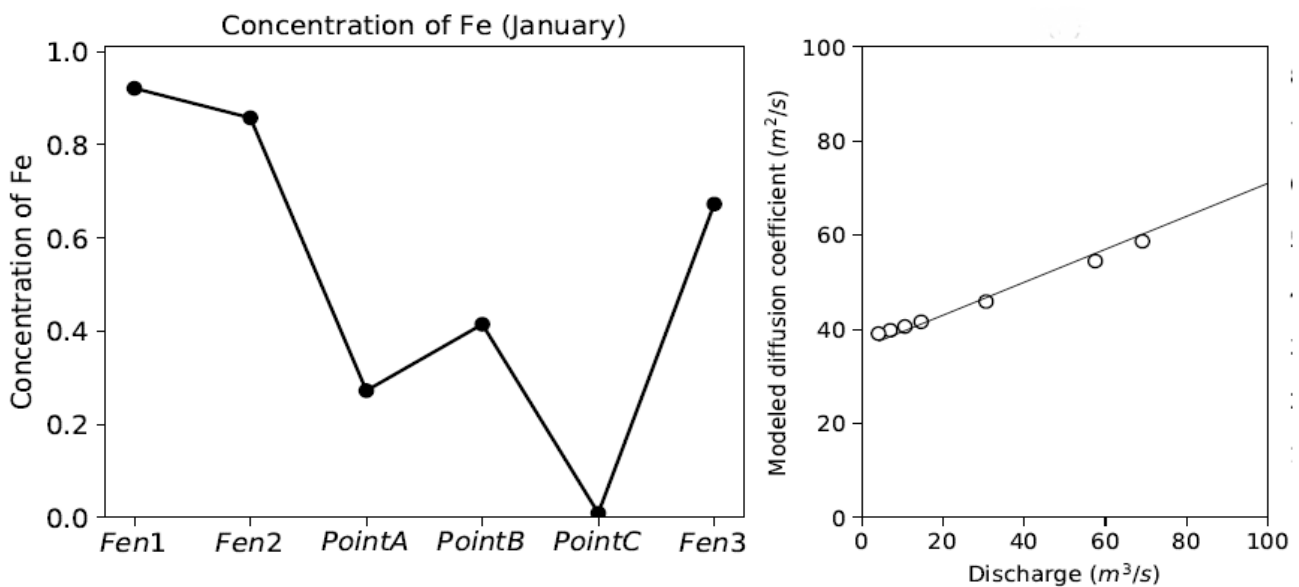


Figure 3: Normalized concentration of Fe in January at all sampling points (left panel) and the right panel shows Diffusion coefficient as a function of discharge from Table 7 (case 2) of Tayfur and Singh (2005) for $D_0 < 100 \text{ m}^2/\text{s}$.

Besides the velocity, the parameter that plays a much more critical role in modeling the transport of pollutants in streams and rivers is the longitudinal diffusion coefficient, D_0 . Once a pollutant is released into a river or flowing water body, it undergoes various stages of mixing with the ambient water. After the contaminant is mixed in the cross-sectional direction, the most important process is the longitudinal dispersion which is measured by the longitudinal dispersion coefficient (Tayfur & Singh, 2005). Tayfur and Singh (2005) developed a model based on Artificial Neural Network (ANN) for predicting the longitudinal dispersion coefficient.

Among other things, they reported that the discharge data alone is sufficient for computing the dispersion coefficient for more frequently occurring low values of the dispersion coefficient $D_0 < 100 \text{ m}^2/\text{s}$. We fitted lines to their data points that are closest to the observed data (see their Table 7, case 2) to get the diffusion coefficient, D , as a function of discharge to be

$$D = 0.35Q + 36 \text{ for } Q \leq 110, \quad (28)$$

as depicted in Figure 3 (right panel). Using the formula in Eq. (28), we estimate the value of the longitudinal dispersion in Fena River to be $39.6 \text{ m}^2/\text{s}$. Thus, the Peclet number is 389 and the parameter $\lambda \approx 194.5$.

Comparison of model results to observational data

We compared the observational data of iron (Fe) concentration in Fena River with the Dirichlet model. The initial concentration $\omega_0=0.52$ is taken to be the average concentration at all locations in January (see Figure 3, left panel). In each case, the inlet boundary is

an exponentially decreasing concentration of the form $\phi_0 e^{-\gamma\tau}$ where $\phi_0=1$. By fitting an exponentially decreasing function to the data at Fen-1 (see Figure 2a), we get $\gamma=0.025$.

We plot the model results against the observational data of Fe in the Fena River for Fen-1, Fen-2, and Point A after estimating all parameters in the analytical solution of the Dirichlet model, Eq. (23). Note that the $e^{-\gamma\tau}$ values are calculated from the dimensionless equation, $\tau=tD_0/L^2$, where $L = 7700 \text{ m}$ is the estimated length scale of the spatial domain.

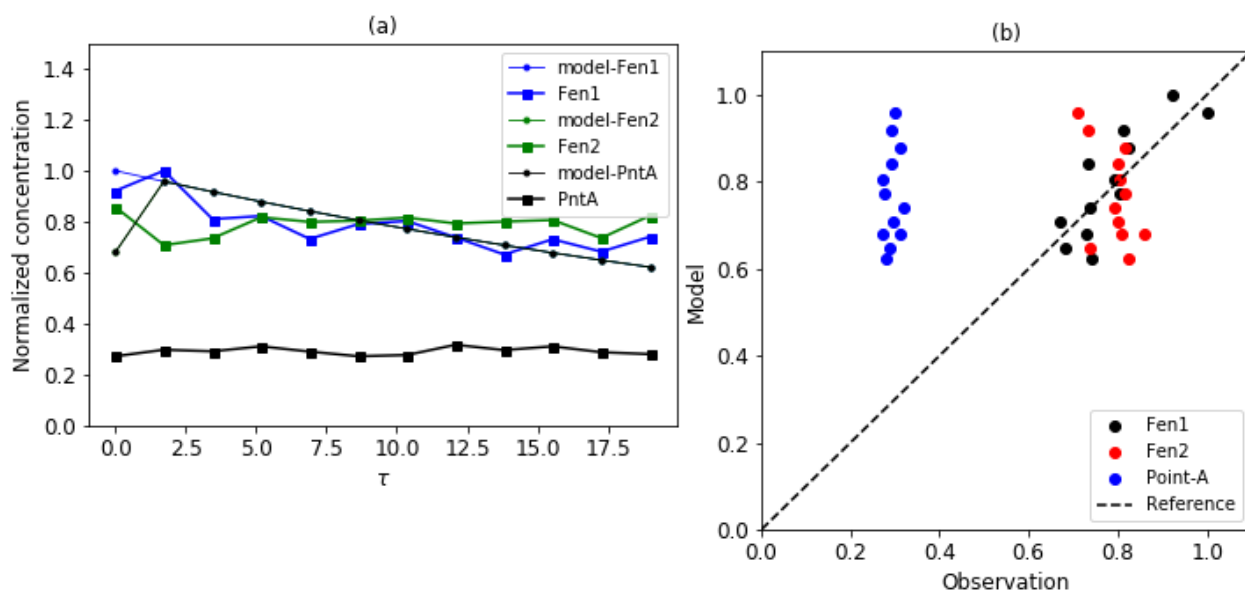


Figure 4: Temporal variation of observed and Dirichlet model concentrations at Fen-1, Fen-2 and Point-A.

The concentration of iron as a function of time from both the observational data and Dirichlet model is shown in Figure 4a. Apart from the initial time, the model results at Fen-1, Fen-2 and Point-A are indistinguishable from each other. The model captures the concentrations at Fen-1 and Fen-2 relatively well since these locations are closer to each other, and data from Fen-1 is used as the inlet boundary condition. However, the model predicts very large concentrations at Point-A. We conjecture a couple of reasons that may account for the higher

modelled concentrations at Point-A. Firstly, Fen-1 and Fen-2 are not directly located on the river, so it is likely that we overestimated the concentrations there, resulting in higher concentrations at Point-A. Secondly, we notice that the normalized concentrations at Point-A are generally constant around a mean value of 0.25 (also see Figure 2f). Thus, it appears other unknown factors, besides direct transport from Fen-1 and Fen-2, maybe implicated. Thirdly, there are several uncertainties in estimating the parameters that went into applying our

model to the observational data. For instance, the speed of the flow varies both in space and time, but this is neither captured in the model nor our observed speed. Finally, another reason could be the fact that the model is one-dimensional and so does not capture lateral dispersion of pollutants which is likely to reduce the concentration of Iron at Point-A if direct transport is the principal mechanism.

The comparison of the Neumann model to the observations is not very different from that of the Dirichlet model, so we do not show that here (see Obeng-Forson, 2022).

Conclusions

We derived analytical solutions to the 1D Advection-Diffusion Equation with exponentially decaying inlet boundary condition. This was motivated by observational data in Fena River in the Ashanti Region of Ghana where illegal mining activities (locally referred to as “galamsey”) have been reported. Using the Laplace transform technique, the analytical solutions were obtained without directly computing the inverse Laplace transform of the transformed equation following work by Kim (2020). Additionally, our analytical solutions were compared to the observed data of pollutants (iron in this case) from Fena River. We found that the analytical results well capture the concentration of iron at two sampling locations, Fen-1 and Fen-2, as shown in Figure 4. However, the model results predicted very large concentrations at Point-A. We have given several reasons that could be responsible for this discrepancy. These include, but not limited to, the fact that (1) the initial source concentrations used in our model might be overestimated, (2) the one-dimensional nature of the model limits lateral dispersion, and (3) other factors, other than direct transport from Fen-1 and Fen-2, might be at play at Point-A. In the future, we plan to model the advection and diffusion of some of the other chemicals found in the river.

References

- Costa, C., Vilhena, M., Moreira, D., & Tirabassi, T. (2006). Semi-analytical solution of the steady three-dimensional advection-diffusion equation in the planetary boundary layer. *Atmospheric Environment*, 40(29):5659–5669.
- Davis, G. (1985). A Laplace transform technique for the analytical solution of a diffusion-convection equation over a finite domain. *Applied Mathematical Modelling*, 9(1):69–71.
- Duncan, A. E. (2020). The Dangerous Couple: Illegal Mining and Water Pollution - A Case Study in Fena River in the Ashanti Region of Ghana. *Journal of Chemistry*.
- Essink, G. H. O. (2001). Improving fresh groundwater supply-problems and solutions. *Ocean & Coastal Management*, 44(5-6):429–449.
- Genuchten, M. T., Leij, F. J., Skaggs, T. H., Toride, N., Bradford, S. A., & Pontedeiro, E. M. (2013). Exact analytical solutions for contaminant transport in rivers 1. the equilibrium advection-dispersion equation. *Journal of Hydrology and Hydromechanics*, 61(2):146.
- Ghanaian Times, (May, 2022). Ghana risks importing water if... <https://www.ghanaiantimes.com.gh/ghana-risk-importing-water-if>.
- Kim, A. S. (2020). Complete analytic solutions for convection-diffusion-reaction-source equations without using an inverse laplace transform. *Scientific Reports*, 10(1):1–13.
- Kumar, A., Jaiswal, D. K., & Yadav, R. R. (2012). Analytical solutions of one-dimensional temporally dependent advection-diffusion equation along longitudinal semi-infinite homogeneous porous domain for uniform flow. *Journal of Mathematics*, 2, 1–11.
- Manitcharoen, N. & Pimpunchat, B. (2020). Analytical and numerical solutions of pollution concentration with uniformly and exponentially increasing forms of sources. *Journal of Applied Mathematics*.

- Mohsen, M. F. N. & Baluch, M. H. (1983). An analytical solution of the diffusion-convection equation over a finite domain. *Applied Mathematical Modelling*, 7(4):285–287.
- Mojtabi, A. & Deville, M. O. (2015). One-dimensional linear advection–diffusion equation: Analytical and finite element solutions. *Computers & Fluids*, 107,189–195.
- Moreira, D., Vilhena, M., Buske, D., & Tirabassi, T. (2006). The giltt solution of the advection–diffusion equation for an inhomogeneous and nonstationary pbl. *Atmospheric Environment*, 40(17):3186–3194.
- Mubarik, A. (2017). *60% of Ghana's water bodies polluted- Water Resources Commission*. Pulse Ghana. <https://www.pulse.com.gh/ece-frontpage/galamsey-60-of-ghanas-water-bodies-polluted-water-resources-commission/czgh6d8>.
- Obeng-Forson, F. (2022). Analytical solutions to 1D advection-diffusion equation and comparison to observations. *MPhil Thesis*, Department of Mathematics, University of Ghana, Legon.
- Ogata, A. & Banks, R. B. (1961). A solution of the differential equation of longitudinal dispersion in porous media: fluid movement in earth materials. *US Government Printing Office*.
- Schaffner, M., Bader, H.-P., & Scheidegger, R. (2009). Modeling the contribution of point sources and non-point sources to thachin river water pollution. *Science of the Total Environment*, 407(17):4902–4915.
- Tayfur, G. & Singh, V. P. R. (2005). Predicting longitudinal dispersion coefficient in natural streams by artificial neural network. *Journal of Hydraulic Engineering*.
- Van Genuchten, M. T. (1982). Analytical solutions of the one- dimensional convective-dispersive solute transport equation. Number 1661. *US Department of Agriculture, Agricultural Research Service*.
- Zoppou, C. & Knight, J. (1997). Analytical solutions for advection and advection-diffusion equations with spatially variable coefficients. *Journal of Hydraulic Engineering*, 123(2):144–148.